Three-beam-interference lithography:
contrast and crystallography

Justin L. Stay and Thomas K. Gaylord*

School of Electrical and Computer Engineering, Georgia Institute of Technology, 777 Atlantic Drive NW, Atlanta,
Georgia 30332-0250, USA

*Corresponding author: tgaylord@ece.gatech.edu

Specific configurations of three linearly polarized, monochromatic plane waves have previously been shown to be capable of producing interference patterns exhibiting symmetry inherent in 5 of the 17 plane groups. Starting with the general expression for N linearly polarized waves, three-beam interference is examined in detail. The totality of all possible sets of constraints for producing the five plane groups is presented. In addition, two uniform contrast conditions are identified and discussed. Further, it is shown that when either of the uniform contrast conditions is applied and the absolute contrast is maximized, unity absolute contrast is achievable.   © 2008 Optical Society of America

OCIS codes: 050.1950, 050.5298, 110.3960, 110.4235, 220.3740, 350.4238.

1. Introduction

Periodic structures such as gratings, photonic crystals, and metamaterials play an important role in advancing optoelectronic technologies. They exhibit useful properties such as diffraction [1], photonic bandgaps [2], and negative refraction [3]. For successful devices and systems, it is imperative that these structures be fabricated accurately, efficiently, and in parallel over an entire substrate or wafer. Multibeam-interference lithography potentially provides such a method for fabricating microscale and nanoscale periodic structures. Using this technique, it is possible for a single photomask (containing numerous diffractive and/or refractive elements) to define a multitude of microscale and nanoscale periodic structures [4]. However, for efficient multibeam lithography to become a reality, a suitably full understanding of multibeam interference must be obtained.

Multibeam interference has been shown to produce all two-dimensional and three-dimensional Bravais lattices [5,6] and 9 of the 17 plane group symmetries using both linearly and elliptically polarized light [7]. In addition, there has been a uniform contrast condition defined [8] to enable generation, when optimized, of high-quality interference patterns (meaning both high absolute contrast and uniform contrast). This results in localized areas of intensity maxima or minima at the lattice points. This is important for two reasons: (1) in lithography, photoresist more readily delineates patterns in response to high-contrast intensity distributions and (2) the resulting intensity distribution will have equal modulation of intensity in multiple basis vector directions through each lattice point. In a fabricated structure defined by three-beam interference, this produces isolated, oval rods (or cavities) at lattice points instead of a continuous structure (or continuous void) between lattice points. At the present time, to the best of the authors' knowledge, a fundamental, systematic, and complete description of the relationship between contrast and symmetry of three-beam interference has not been presented in the literature.

Starting with the general expression for N linearly polarized waves, the three-beam interference case is examined in detail. The totality of all possible sets of conditions for producing the five plane groups that are possible with linearly polarized plane waves is

presented. These conditions are given in terms of the set of basis vectors defining the translational symmetry of the lattice and the interference coefficients appearing in the general expression. In addition, two uniform contrast conditions are identified and discussed. For both conditions, the requirements to achieve unity absolute contrast are presented. Each of the five plane groups is discussed in detail in terms of its symmetry elements, range of contrast, maximum contrast, specific configurations, and interference patterns typical of each plane group.

2. Multibeam Interference

In order to understand how design parameters affect the resulting interference patterns, an expression for the intensity distribution is needed. First, an expression for the interference of N linearly polarized, monochromatic plane waves is developed. The electric field of the ith plane wave can be represented in terms of its complex vector phasor, $\mathbf{E}_i$, angular frequency, ω, and initial phase, ϕ_i, as $\mathcal{E}_i(\mathbf{r},t) = \mathbf{Re}[\mathbf{E}_i(\mathbf{r})\exp(j\omega t)]$, where its complex vector phasor is $\mathbf{E}_i(\mathbf{r}) = E_i\exp[-j(\mathbf{k}_i\cdot\mathbf{r} - \phi_i)]\hat{\mathbf{e}}_i$. The time average intensity distribution for a single monochromatic plane wave, I_i, is related to the square of the electric field. This intensity can be expressed as

$$I_i(\mathbf{r}) = \langle\mathcal{E}_i(\mathbf{r},t)\cdot\mathcal{E}_i(\mathbf{r},t)\rangle$$
$$= \frac{1}{2}\mathbf{Re}[\mathbf{E}_i(\mathbf{r})\cdot\mathbf{E}_i^*(\mathbf{r})]$$
$$= \frac{1}{2}E_i^2. \qquad (1)$$

For the interference of two linearly polarized, monochromatic plane waves, the total complex electric field phasor is $\mathbf{E}_T(\mathbf{r}) = \mathbf{E}_1(\mathbf{r}) + \mathbf{E}_2(\mathbf{r})$. The time average intensity distribution for the interference pattern, I_T, is related to the square of the total electric field as

$$I_T(\mathbf{r}) = \langle\mathcal{E}_T(\mathbf{r},t)\cdot\mathcal{E}_T(\mathbf{r},t)\rangle$$
$$= I_1(\mathbf{r}) + I_2(\mathbf{r}) + 2J_{12}(\mathbf{r}), \qquad (2)$$

where the interference term, J_{12}, is defined as

$$J_{12}(\mathbf{r}) = \langle\mathcal{E}_1(\mathbf{r},t)\cdot\mathcal{E}_2(\mathbf{r},t)\rangle$$
$$= \frac{1}{2}\mathbf{Re}[\mathbf{E}_1(\mathbf{r})\cdot\mathbf{E}_2^*(\mathbf{r})]$$
$$= \frac{1}{2}E_1E_2e_{12}\cos((\mathbf{k}_2 - \mathbf{k}_1)\cdot\mathbf{r} + \phi_1 - \phi_2), \qquad (3)$$

and the efficiency factor, e_{12}, is defined as $e_{12} = \hat{\mathbf{e}}_1\cdot\hat{\mathbf{e}}_2$. For the interference of N linearly polarized, monochromatic plane waves, the time average intensity

distribution can be expressed as

$$I_T(\mathbf{r}) = \langle\mathcal{E}_T(\mathbf{r},t)\cdot\mathcal{E}_T(\mathbf{r},t)\rangle$$
$$= \sum_{i=1}^{N}\left(I_i(\mathbf{r}) + \sum_{j>i}^{N}2J_{ij}(\mathbf{r})\right)$$
$$= \sum_{i=i}^{N}\left(\frac{1}{2}E_i^2 + \sum_{j>i}^{N}E_iE_je_{ij}\cos((\mathbf{k}_j - \mathbf{k}_i)\cdot\mathbf{r}$$
$$+ \phi_i - \phi_j)\right). \qquad (4)$$

Equation (4) represents the three-dimensional interference pattern for N linearly polarized, monochromatic plane waves. Proper selection of wave vectors ($\mathbf{k}_i$), polarization states ($\hat{\mathbf{e}}_i$), and electric field amplitudes (E_i) can produce interference patterns with a wide range of contrast and plane group symmetries. Generally, these should be chosen such that the configuration produces a high-quality interference pattern.

3. Three-Beam Interference

In general, interference of three linearly polarized plane waves will produce an interference pattern invariant in the z direction. Primitive basis vectors ($\mathbf{a}$ and $\mathbf{b}$) in the xy plane define the translational symmetry of the interference pattern. The reciprocal lattice vectors ($\mathbf{A}$ and $\mathbf{B}$) can be expressed as

$$\mathbf{A} = 2\pi\frac{\mathbf{b}\times\hat{\mathbf{z}}}{\mathbf{a}\cdot\mathbf{b}\times\hat{\mathbf{z}}}, \qquad \mathbf{B} = 2\pi\frac{\hat{\mathbf{z}}\times\mathbf{a}}{\mathbf{a}\cdot\mathbf{b}\times\hat{\mathbf{z}}}. \qquad (5)$$

For three-beam interference, the three recording wave vectors can be found by finding the circumcenter vector ($\mathbf{P}$) of a triangle defined by the two reciprocal lattice vectors in Eqs. (5). The projections of the recording wave vectors on the xy plane are then defined as vectors from the circumcenter to each vertex such that $\mathbf{k}_{1,xy} = -\mathbf{P}$, $\mathbf{k}_{2,xy} = \mathbf{A} - \mathbf{P}$, and $\mathbf{k}_{3,xy} = \mathbf{B} - \mathbf{P}$. The z component of the individual wave vectors are adjusted accordingly such that $|\mathbf{k}_i| = nk_o$, where $k_o = 2\pi/\lambda$ and n is the index of refraction of the recording medium. In general, the relationship between the set of basis vectors and the recording wavelength is

$$\frac{\lambda}{n} \leq \frac{2\sin^2\gamma}{\left(\dfrac{1}{|\mathbf{a}|^2} + \dfrac{1}{|\mathbf{b}|^2} + \dfrac{2\cos\gamma}{|\mathbf{a}||\mathbf{b}|}\right)^{1/2}}, \qquad (6)$$

where γ is the angle between $\mathbf{a}$ and $\mathbf{b}$. The effect of Eq. (6) must be fully understood. A given two-dimensional lattice has an infinite number of sets of primitive basis vectors that can define the translation symmetry of the that lattice. Given the methodology above, two sets of primitive basis vectors that define the same translational symmetry will not provide an identical set of recording wave vectors. While the translational symmetry of the interference

patterns will be identical, the locations of other symmetry elements will differ. Thus, given the methodology above, the choice of **a** and **b** corresponds not only to a particular translational symmetry of the final interference pattern, but also to other symmetry elements and their locations within a primitive unit cell.

Equation (4) can be simplified for the three-beam case. Without losing a general sense of the isointensity contours of the interference pattern, the initial phases of the interfering beams can be set to zero ($\phi_i = 0$) if no two interfering wave vectors are equal. With this assumption, Eq. (4) reduces to

$$I_T = I_0[1 + V_{12} \cos(\mathbf{G}_{21} \cdot \mathbf{r}) + V_{13} \cos(\mathbf{G}_{31} \cdot \mathbf{r}) + V_{23} \cos(\mathbf{G}_{32} \cdot \mathbf{r})], \tag{7}$$

where

$$I_0 = \frac{1}{2} \sum_{k=1}^{3} E_k^2, \tag{8}$$

the interference coefficient is

$$V_{ij} = \frac{E_i E_j e_{ij}}{I_0}, \tag{9}$$

and $\mathbf{G}_{ij} = \mathbf{k}_i - \mathbf{k}_j$. It should be noted that the desired reciprocal lattice vectors (**A** and **B**) correspond to $\mathbf{G}_{21}$ and $\mathbf{G}_{31}$, respectively, in Eq. (7), while $\mathbf{G}_{32}$ is a dependent reciprocal lattice vector, defined as ($\mathbf{G}_{31} - \mathbf{G}_{21}$) or (**B** − **A**).

4. Contrast and Crystallography

Of the 17 plane symmetry groups, five can be realized through the interference of three linearly polarized plane waves [7]. These are the *p2*, *pmm*, *cmm*, *p4m*, and *p6m* plane symmetry groups. Here we analyze each of the five plane symmetry groups and discuss how contrast affects the overall quality of the interference pattern produced.

Absolute contrast (V_{abs}) is a function of the intensity extrema in an intensity distribution and is defined as

$$V_{\text{abs}} = \frac{I_{\max} - I_{\min}}{I_{\max} + I_{\min}}, \tag{10}$$

where $I_{\max}$ and $I_{\min}$ are the maximum and minimum intensities, respectively. Two equivalent primitive unit cell representations are used in this work: (1) the conventional primitive unit cell defined by **a** and **b** and (2) the Wigner–Seitz proximity primitive unit cell whose sides are perpendicular bisectors of the shortest lattice vectors. The boundaries of the conventional unit cell and the proximity unit cell will be shown in the subsequent figures as dashed and dotted lines, respectively. The latter are centered at **r** = 0. All of the *xy* plane can be filled by either unit cell with translations by integer combinations of the primitive basis vectors. Each primitive unit cell

contains all of the information about the interference pattern. Consistent with the previous assumption that $\phi_i = 0$, an intensity maximum or minimum occurs at the **r** = 0 lattice point (and consequently at all lattice points throughout the interference pattern).

The quality of the interference pattern can be improved by applying and optimizing one of two uniform contrast conditions. High-quality patterns will have high absolute contrast and exhibit uniform contrast. This results in localized areas of intensity extrema at the lattice points. This is important for two reasons: (1) in lithography, photoresist more readily delineates patterns in response to high-contrast intensity distributions and (2) the resulting intensity distribution will have equal modulation of intensity in multiple basis vector directions through each lattice point. In a fabricated structure defined by three-beam interference, this produces isolated, oval rods (or cavities) at lattice points instead of a continuous structure (or continuous void) between lattice points.

The first uniform contrast condition (UCC-1) can be applied by choosing the plane wave properties such that the three interference coefficients (V_{ij}) in Eq. (7) are equal [8]. The interference coefficient ($V^{(1)}$) is defined as

$$V^{(1)} = V_{12} = V_{13} = V_{23}. \tag{11}$$

This condition of uniform contrast guarantees that at each lattice point, an equal modulation of intensity occurs in three lattice directions (**a**, **b**, and **a** + **b**). It also dictates that the other, opposite intensity extrema will lie at $(2/3)\mathbf{a} + (1/3)\mathbf{b}$ and $(1/3)\mathbf{a} + (2/3)\mathbf{b}$ from each lattice point. This corresponds to the centroids of three lattice points defined by two sets of vectors, the first being **a** and **a** + **b** and the second being **b** and **a** + **b**. For three-beam interference, there exist constraints on the electric field amplitudes, E_i, as a function of the polarization states, $\hat{\mathbf{e}}_i$, for UCC-1 to be satisfied. The constraints are [5]

$$E_2 = \frac{e_{13}}{e_{23}} E_1, \qquad E_3 = \frac{e_{12}}{e_{23}} E_1. \tag{12}$$

When the constraints in Eqs. (12) are satisfied, Eq. (11) can be simplified to

$$V^{(1)} = \frac{2 e_{12} e_{13} e_{23}}{e_{12}^2 + e_{13}^2 + e_{23}^2}. \tag{13}$$

There exists a relationship between the interference coefficient ($V^{(1)}$) and the absolute contrast (V_{abs}). For three-beam interference, the relationship is

$$V_{\text{abs}} = \left| \frac{9}{4/V^{(1)} + 3} \right|. \tag{14}$$

In summary, UCC-1 is defined as follows:

UCC-1 is satisfied when the parameters of the three recording beams are chosen such that all three interference coefficients (V_{ij}) are equal. This results in an interference pattern in which (1) from each lattice point, there is equal modulation of intensity in the **a**, **b**, and **a** + **b** directions, and (2) in each primitive unit cell there is one intensity maxima (minima) located at the lattice point and two equivalent intensity minima (maxima) at $(2/3)\mathbf{a} + (1/3)\mathbf{b}$ and $(1/3)\mathbf{a} + (2/3)\mathbf{b}$ from the lattice point.

The second uniform contrast condition (UCC-2) can be applied by choosing the plane wave properties such that two of the interference coefficients in Eq. (7) are equal and the third is zero. For example,

$$V^{(2)} = V_{12} = V_{13}, \qquad V_{23} = 0. \qquad (15)$$

This condition of uniform contrast guarantees that at each lattice point, an equal modulation of intensity occurs in two primitive lattice directions (**a** and **b**). It also dictates that the other, opposite intensity extrema will lie at $(1/2)\mathbf{a} + (1/2)\mathbf{b}$ from each lattice point. This corresponds to the centroid of a parallelogram defined by the set of vectors **a** and **b**. For three-beam interference, there exist constraints on the polarization states, $\hat{\mathbf{e}}_i$, and electric field amplitudes, E_i, for this uniform contrast condition to be satisfied. The constraints are

$$e_{23} = 0, \qquad E_3 = \frac{e_{12}}{e_{13}}E_2. \qquad (16)$$

When the constraints in Eq. (16) are satisfied, Eq. (9) simplifies to

$$V^{(2)} = \frac{2E_1E_2e_{12}e_{13}^2}{E_1^2e_{13}^2 + E_2^2e_{13}^2 + E_2^2e_{12}^2}. \qquad (17)$$

There exists a relationship between the interference coefficient ($V^{(2)}$) and the absolute contrast (V_{abs}). For three-beam interference, the relationship is

$$V_{abs} = |2V^{(2)}|. \qquad (18)$$

In summary, UCC-2 is defined as follows:

UCC-2 is satisfied when the parameters of the three recording beams are chosen such that two interference coefficients (V_{ij}) are equal and the third is zero. With $V_{23} = 0$, this results in an interference pattern in which (1) from each lattice point, there is equal modulation of intensity in the **a** and **b** directions and (2) in each primitive unit cell there is one intensity maxima (minima) located at the lattice point and one intensity minima (maxima) at $(1/2)\mathbf{a} + (1/2)\mathbf{b}$ from the lattice point.

It should be noted that UCC-2 can be applied with two other sets of constraints. While it was arbitrarily chosen to set $V_{23} = 0$, either of the other two inter-

ference coefficients can be set to zero. However, the description for the locations of the other intensity extrema and directions of equal modulation of intensity will differ. In the discussions following, references to UCC-2 will assume the derivation above.

While these uniform contrast conditions guarantee equal modulation of intensity in specific lattice directions, maximization of the absolute contrast in Eqs. (14) and (18) is a separate operation. This corresponds to either the maximization or minimization of the interference coefficient ($V^{(1)}$ or $V^{(2)}$). Solutions with values of $V^{(1)} = 2/3$ or $V^{(1)} = -1/3$ for UCC-1 and values of $V^{(2)} = 1/2$ or $V^{(2)} = -1/2$ for UCC-2 result in unity absolute contrast ($V_{abs} = 1$); however, this may not always be achievable. An optimal solution is one that maximizes absolute contrast while satisfying one of the two uniform contrast conditions. This ensures that the interference pattern produced can be easily imaged in a photosensitive material. In general, this process of maximizing the contrast can be performed through constrained nonlinear optimization. As derived above, absolute contrast (V_{abs}) is related to the interference coefficient ($V^{(1)}$ or $V^{(2)}$) when a uniform contrast condition is satisfied. Maximization or minimization of the interference coefficient will in turn maximize absolute contrast. Modern personal computers are able to perform this optimization in a few seconds.

Finding an optimal solution that satisfies UCC-1 is more involved than for UCC-2, because there exist two fundamentally different types of interference patterns that result from satisfying this uniform contrast condition. These two cases can be identified by the sign of the interference coefficient ($V^{(1)}$) from Eq. (13). If a solution is found such that the sign of $V^{(1)}$ is positive, maximum intensity extrema will be located at the lattice points. Conversely, if a solution is found such that the sign of $V^{(1)}$ is negative, minimum intensity extrema will be located at the lattice points. Considering all possible solutions to Eq. (13) for optimal values of the interference coefficient ($V^{(1)} = 2/3$ or $V^{(1)} = -1/3$) subject to the allowed values of the efficiency terms (e_{ij}), given by the inequalities

$$|e_{13} + e_{23}| \leq 2\cos\left(\frac{\cos^{-1}(e_{12})}{2}\right), \qquad (19)$$

$$|e_{12} + e_{23}| \leq 2\cos\left(\frac{\cos^{-1}(e_{13})}{2}\right), \qquad (20)$$

$$|e_{12} + e_{13}| \leq 2\cos\left(\frac{\cos^{-1}(e_{23})}{2}\right), \qquad (21)$$

there exists only two sets of solutions to obtain unity absolute contrast. For $V^{(1)} = 2/3$, unity absolute contrast occurs when the solution satisfies the following (corresponding to four solutions—all signs are positive or two signs are negative):

$$e_{12} = \pm1, \qquad e_{13} = \pm1, \qquad e_{23} = \pm1. \qquad (22)$$

This results in electric field amplitudes of

$$E_2 = \pm E_1, \qquad E_3 = \pm E_1. \tag{23}$$

This solution describes an impractical configuration for three-beam interference in which all recording wave vectors are coplanar, and it is not necessarily achievable. Thus, in general, an optimization must be performed to solve for a solution that maximizes absolute contrast for $V^{(1)} > 0$.

For $V^{(1)} = -1/3$, unity absolute contrast occurs when the solution satisfies the following (corresponding to four solutions—all signs are negative or two signs are positive):

$$e_{12} = \pm\frac{1}{2}, \qquad e_{13} = \pm\frac{1}{2}, \qquad e_{23} = \pm\frac{1}{2}. \tag{24}$$

This results in electric field amplitudes of

$$E_2 = \pm E_1, \qquad E_3 = \pm E_1. \tag{25}$$

The physical representation of Eq. (24) implies that all three of the polarization vectors are coplanar and make equal angles (120°) with one another (or some variant of the individual polarizations vectors, $\hat{e}_i$, and their inversions, $-\hat{e}_i$). In general, there always exist solutions of this form in which unity absolute contrast is achieved ($V_{abs} = 1$) while satisfying UCC-1 for $V^{(1)} = -1/3$. This can be proved by using the following approach. In an arbitrary case, k_1 and k_2 represent two of the three recording wave vectors. All combinations of polarizations, $\hat{e}_1$ and $\hat{e}_2$, such that $e_{12} = 1/2$ can be found. For each combination, a third polarization vector, $\hat{e}_3$, can be calculated such that $e_{13} = e_{23} = 1/2$. These calculated polarization vectors, for $\hat{e}_3$, will trace out a line in three-dimensional space such the polarization space of any third recording wave vector will include at least two points on this line, each corresponding to a solution that satisfies UCC-1 and unity absolute contrast is achieved.

Finding an optimal solution that satisfies UCC-2 is performed similarly. Considering all possible solutions to Eq. (17) for optimal values of the interference coefficient ($V^{(2)} = \pm 1/2$) subject to the allowed values of the efficiency terms (e_{ij}), given by the inequality

$$|e_{12} + e_{13}| \le \sqrt{2}/2, \tag{26}$$

there exists only one set of solutions to obtain unity absolute contrast. This occurs when the solution satisfies the following (corresponding to four solutions):

$$e_{12} = \pm\frac{\sqrt{2}}{2}, \qquad e_{13} = \pm\frac{\sqrt{2}}{2}, \qquad e_{23} = 0. \tag{27}$$

This results in electric field amplitudes of

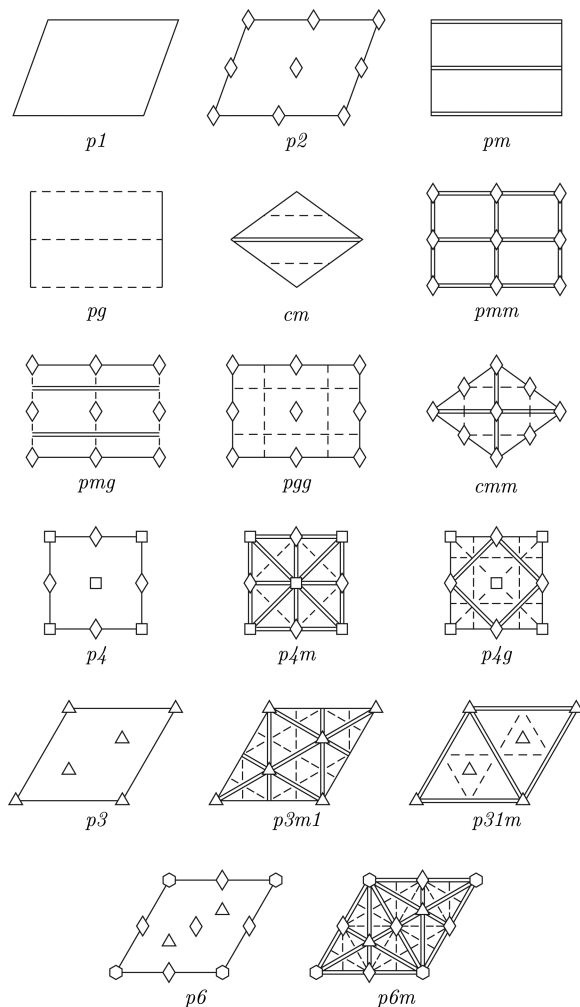$$E_2 = \pm\frac{\sqrt{2}}{2}E_1, \qquad E_3 = \pm\frac{\sqrt{2}}{2}E_1. \tag{28}$$

The physical representation of Eq. (27) implies that all three of the polarization vectors are coplanar, such that $\hat{e}_2$ and $\hat{e}_3$ are orthogonal and $\hat{e}_1$ bisects the other two (or some variant of the individual polarizations vectors, $\hat{e}_i$, and their inversions, $-\hat{e}_i$). In general, there always exist solutions of this form in which unity absolute contrast is achieved ($V_{abs} = 1$) while satisfying UCC-2 for $V^{(2)} = \pm 1/2$. This can be proved by using a methodology similar to that above.

Finding solutions that exhibit unity absolute contrast ($V_{abs} = 1$, $I_{min} = 0$) that satisfy UCC-1 (with $V^{(1)} < 0$) or UCC-2 relies on total destructive interference. This ensures that at some points in space $I_T = 0$. However, this occurs for only one of two fundamentally different interference patterns when absolute contrast is maximized while satisfying UCC-1. The sign of $V^{(2)}$ does not distinguish between different types of interference patterns for UCC-2 because the contours of the motifs around intensity maxima and minima are identical for values of $V^{(2)}$ and $-V^{(2)}$. It does, however, determine whether an intensity maxima ($V^{(2)} > 0$) or minima ($V^{(2)} < 0$) is located at a lattice point. This distinction based on the sign of the interference coefficient is similar to the use of dark and light field masks in conventional lithography. The choice of one type of interference pattern over another (or the use of dark or light field masks) will depend on process parameters. However, maximizing absolute contrast for UCC-1 with $V^{(1)} > 0$ is more complicated, and explicit solutions can be expressed only in a few situations of higher-order symmetry.

5. Plane Symmetry Group p2

The *p2* plane symmetry group is obtained from general three-beam interference. This plane group is characterized as having four unique points of twofold symmetry as shown in Fig. 1. This figure illustrates the symmetry elements and their general locations for each of the 17 plane groups [8]. Of these, interference patterns of three linearly polarized plane waves can exhibit five of these symmetry groups, while an additional four are possible if elliptical polarization is available [7]. Figure 1 can be used to identify the symmetry elements present in any two-dimensional interference pattern.

Higher-order symmetry groups will emerge as relationships between primitive basis vectors and interference coefficients vary. The values of contrast for interference patterns with this symmetry range from 0 to 1 depending on the constraints applied. However, both uniform contrast conditions can be applied and absolute contrast maximized to obtain unity absolute contrast ($V_{abs} = 1$), provided sets of constraints are not satisfied for higher-order plane groups. Contrast for interference patterns with higher-order symmetries will be discussed in more detail below.

Fig. 1. Locations of symmetry elements for the 17 plane groups [9]. Unit cell outlines correspond to conventional primitive unit cells, illustrated in subsequent figures as dashed lines.

Centers of Rotation

◇ 2-fold   ▭ Reflection axis
△ 3-fold   ------- Glide-reflection axis
□ 4-fold   —— Unit cell outline
○ 6-fold

pmm

$$\mathbf{a} = (\tfrac{3}{2}\lambda, 0, 0) \quad \mathbf{k}_1 = k_o(-\tfrac{1}{3}, -\tfrac{1}{2}, -\tfrac{\sqrt{23}}{6})$$
$$\mathbf{b} = (0, \lambda, 0) \quad \mathbf{k}_2 = k_o(\tfrac{1}{3}, -\tfrac{1}{2}, -\tfrac{\sqrt{23}}{6})$$
$$V_{abs} = 1 \quad \mathbf{k}_3 = k_o(-\tfrac{1}{3}, \tfrac{1}{2}, -\tfrac{\sqrt{23}}{6})$$
$$V^{(2)} = \tfrac{1}{2} \quad \hat{\mathbf{e}}_1 = (0.4303, 0.6737, -0.6009)$$
$$E_2 = -\tfrac{\sqrt{2}}{2}E_1 \quad \hat{\mathbf{e}}_2 = (0.3329, -0.7308, 0.5960)$$
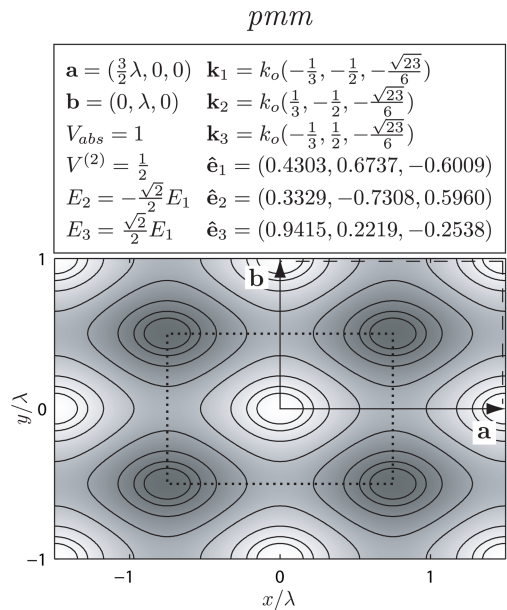$$E_3 = \tfrac{\sqrt{2}}{2}E_1 \quad \hat{\mathbf{e}}_3 = (0.9415, 0.2219, -0.2538)$$

Fig. 2. Design parameters and associated interference pattern exhibiting *pmm* plane group symmetry. The UCC-2 has been applied and absolute contrast maximized, resulting in unity absolute contrast ($V_{\mathrm{abs}} = 1$), with zero intensity at intensity nulls. The conventional primitive unit cell (dashed lines) and the Wigner–Seitz proximity unit cell (dotted lines) are shown.

is applied until parameters satisfy constraints for the *p4m* plane symmetry group, which arises when UCC-2 is applied and a set of primitive basis vectors (**a** and **b**, **a** and **a** + **b**, or **a** + **b** and **b**) are equal in magnitude. Typical interference patterns exhibiting *pmm* plane group symmetry can be seen in Figs. 2 and 3 along with the corresponding design parameters.

pmm

$$\mathbf{a} = (\tfrac{3}{2}\lambda, 0, 0) \quad \mathbf{k}_1 = k_o(-\tfrac{1}{3}, -\tfrac{1}{2}, -\tfrac{\sqrt{23}}{6})$$
$$\mathbf{b} = (0, \lambda, 0) \quad \mathbf{k}_2 = k_o(\tfrac{1}{3}, -\tfrac{1}{2}, -\tfrac{\sqrt{23}}{6})$$
$$V_{abs} = 0.585 \quad \mathbf{k}_3 = k_o(-\tfrac{1}{3}, \tfrac{1}{2}, -\tfrac{\sqrt{23}}{6})$$
$$V = N/A \quad \hat{\mathbf{e}}_1 = (0.4303, 0.6737, -0.6009)$$
$$E_2 = -\tfrac{\sqrt{2}}{2}E_1 \quad \hat{\mathbf{e}}_2 = (0.3329, -0.7308, 0.5960)$$
$$E_3 = \tfrac{5}{2}E_1 \quad \hat{\mathbf{e}}_3 = (0.9415, 0.2219, -0.2538)$$

Fig. 3. Design parameters and associated interference pattern exhibiting *pmm* plane group symmetry. No uniform contrast condition has been applied. The conventional primitive unit cell (dashed lines) and the Wigner–Seitz proximity unit cell (dotted lines) are shown.

6. Plane Symmetry Group *pmm*

The *pmm* symmetry group is the next higher symmetry plane group obtainable with three-beam-interference lithography. This plane group is characterized as having four unique reflection axes and four unique points of twofold symmetry as shown in Fig. 1. This plane symmetry group can be realized when plane wave parameters are chosen such that they satisfy one of three sets of constraints: (1) $V_{23} = 0$ ($e_{23} = 0$) and $\mathbf{a} \cdot \mathbf{b} = 0$, (2) $V_{12} = 0$ ($e_{12} = 0$) and $\mathbf{a} \cdot (\mathbf{a} + \mathbf{b}) = 0$, or (3) $V_{13} = 0$ ($e_{13} = 0$) and $\mathbf{b} \cdot (\mathbf{a} + \mathbf{b}) = 0$. When one of these sets of constraints is satisfied, only two of the three interference terms are present in Eq. (7), and the corresponding reciprocal wave vectors ($\mathbf{G}_{ij}$) are orthogonal. Ensuring that $V_{ij} = 0$ is not the only constraint for UCC-2. However, this symmetry can still exist when UCC-2

The interference patterns illustrated in this paper are constructed such that a full range of isointensity contours can be observed. Overlain on these contour plots are normalized, semitransparent gray-scale images of the interference patterns. These, however, are to illustrate locations of intensity extrema and not an indication of actual absolute contrast.

Situations in both figures begin with an identical set of basis vectors and identical polarization unit vectors. Figure 2 satisfies UCC-2, while Fig. 3 does not satisfy any uniform contrast condition. Since UCC-2 is applied and absolute contrast is maximized in Fig. 2, it exhibits unity absolute contrast ($V_{abs} = 1$) with an interference coefficient $V^{(2)} = 1/2$. Figure 3 does not satisfy a uniform contrast condition and has an absolute contrast of $V_{abs} = 0.585$. For the pmm plane group, absolute contrast can vary from 0 to 1 depending on the chosen plane wave parameters. However, when UCC-2 can be applied and absolute contrast is maximized, unity absolute contrast ($V_{abs} = 1$) can always be achieved.

7. Plane Symmetry Group *cmm*

The cmm symmetry group (along with the pmm plane symmetry group) is the next higher symmetry group after $p2$. This plane group is characterized as having two unique reflection axes, two unique glide reflection axes, and four unique points of twofold symmetry as shown in Fig. 1. This plane symmetry group can be realized when plane wave parameters are chosen such that they satisfy one of three sets of constraints: (1) $V_{12} = V_{13}$ and $|\mathbf{a}| = |\mathbf{b}|$, (2) $V_{13} = V_{23}$ and $|\mathbf{a}| = |\mathbf{a} + \mathbf{b}|$, or (3) $V_{12} = V_{23}$ and $|\mathbf{b}| = |\mathbf{a} + \mathbf{b}|$. When one of these sets of constraints is satisfied, all three interference terms may be present. Two of the three corresponding reciprocal wave vectors ($\mathbf{G}_{ij}$) will be equal in magnitude, while the third (if present) will be an exterior bisector of the previous two. This symmetry will still exist when both uniform contrast conditions are applied until parameters satisfy constraints for either the $p4m$ or $p6m$ plane symmetry groups. The $p6m$ plane group will emerge when UCC-1 is applied and a set of primitive basis vectors (**a** and **b**) make an angle of $120°$ with one another. The $p4m$ plane group will emerge when UCC-2 is applied and a set of primitive basis vectors (**a** and **b**, **a** and **a** + **b**, or **a** + **b** and **b**) make an angle of $90°$ with one another. Typical interference patterns with cmm plane group symmetry are illustrated in Figs. 4 and 5 along with the corresponding design parameters.
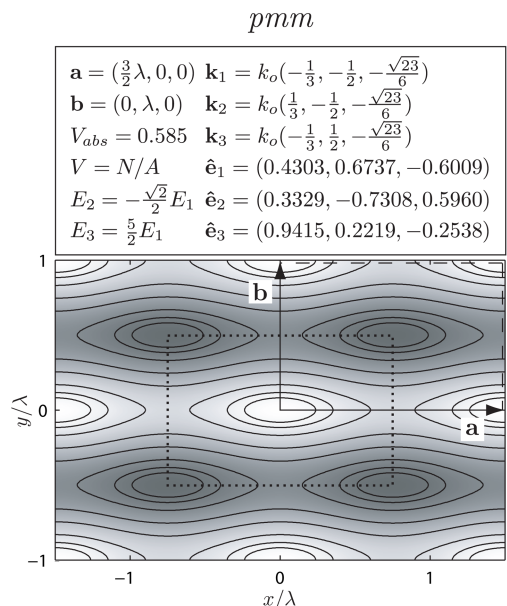
The design in Fig. 4 satisfies UCC-1, while Fig. 5 satisfies UCC-2. Figure 4 illustrates one of the two fundamentally different interference patterns possible with the application of UCC-1, exhibiting peaks of intensity at lattice points. It has an absolute contrast (V_{abs}) of 0.8946 and an interference coefficient $V^{(1)} = 0.5666$. This design is optimized for this type of interference pattern, for $V^{(1)} > 0$. However, if we allow $V^{(1)} < 0$, there exists a solution such that unity absolute contrast ($V_{abs} = 1$) is achieved. Figure 5

cmm

$\mathbf{a} = (\lambda, 0, 0)$ $\quad \mathbf{k}_1 = k_o(-\frac{1}{2}, -\frac{1}{2}, -\frac{\sqrt{2}}{2})$
$\mathbf{b} = (0, \lambda, 0)$ $\quad \mathbf{k}_2 = k_o(\frac{1}{2}, -\frac{1}{2}, -\frac{\sqrt{2}}{2})$
$V_{abs} = 0.8946$ $\quad \mathbf{k}_3 = k_o(-\frac{1}{2}, \frac{1}{2}, -\frac{\sqrt{2}}{2})$
$V^{(1)} = 0.5666$ $\quad \hat{\mathbf{e}}_1 = (\frac{1}{2}, \frac{1}{2}, -\frac{\sqrt{2}}{2})$
$E_2 = 0.9419 E_1$ $\quad \hat{\mathbf{e}}_2 = (0.4967, 0.8344, -0.2388)$
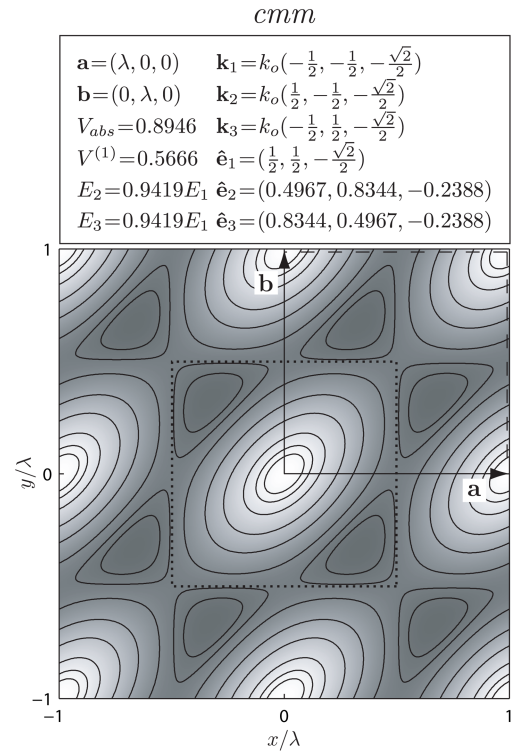$E_3 = 0.9419 E_1$ $\quad \hat{\mathbf{e}}_3 = (0.8344, 0.4967, -0.2388)$

Fig. 4. Design parameters and associated interference pattern exhibiting cmm plane group symmetry. This design results in one of two fundamentally different interference patterns when UCC-1 is applied, possessing intensity peaks at lattice points. The conventional primitive unit cell (dashed lines) and the Wigner–Seitz proximity unit cell (dotted lines) are shown.
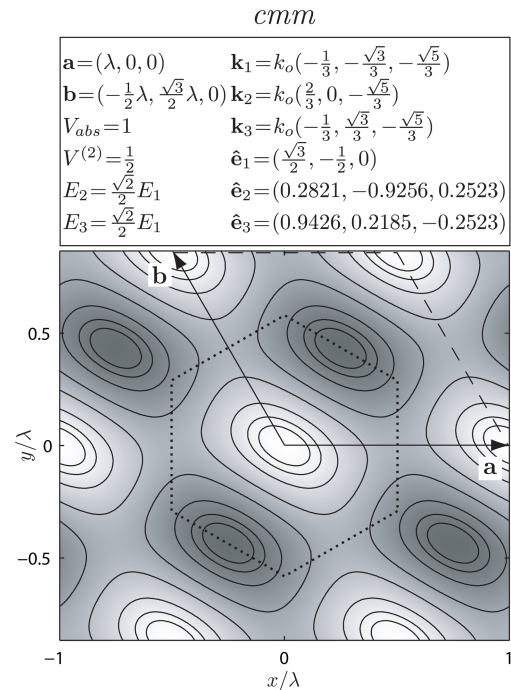

cmm

$\mathbf{a} = (\lambda, 0, 0)$ $\quad \mathbf{k}_1 = k_o(-\frac{1}{3}, -\frac{\sqrt{3}}{3}, -\frac{\sqrt{5}}{3})$
$\mathbf{b} = (-\frac{1}{2}\lambda, \frac{\sqrt{3}}{2}\lambda, 0)$ $\quad \mathbf{k}_2 = k_o(\frac{2}{3}, 0, -\frac{\sqrt{5}}{3})$
$V_{abs} = 1$ $\quad \mathbf{k}_3 = k_o(-\frac{1}{3}, \frac{\sqrt{3}}{3}, -\frac{\sqrt{5}}{3})$
$V^{(2)} = \frac{1}{2}$ $\quad \hat{\mathbf{e}}_1 = (\frac{\sqrt{3}}{2}, -\frac{1}{2}, 0)$
$E_2 = \frac{\sqrt{2}}{2} E_1$ $\quad \hat{\mathbf{e}}_2 = (0.2821, -0.9256, 0.2523)$
$E_3 = \frac{\sqrt{2}}{2} E_1$ $\quad \hat{\mathbf{e}}_3 = (0.9426, 0.2185, -0.2523)$

Fig. 5. Design parameters and associated interference pattern exhibiting pmm plane group symmetry. The UCC-2 has been applied and absolute contrast maximized, resulting in unity absolute contrast ($V_{abs} = 1$), with zero intensity at intensity nulls. The conventional primitive unit cell (dashed lines) and the Wigner–Seitz proximity unit cell (dotted lines) are shown.

illustrates a design with unity absolute contrast ($V_{abs} = 1$) and an interference coefficient $V^{(2)} = 1/2$. Like the *pmm* plane group, absolute contrast can vary from 0 to 1 depending on the chosen plane wave parameters. However, when UCC-1 and UCC-2 can be applied, unity absolute contrast ($V_{abs} = 1$) can always be achieved.

8. Plane Symmetry Group *p4m*

The *p4m* plane symmetry group is the next higher symmetry group after *cmm* and *pmm*. This plane group is characterized as having six unique reflection axes, two unique glide reflection axes, two fourfold symmetry points, and two twofold symmetry points as shown in Fig. 1. This plane symmetry group can be realized when plane wave parameters are chosen such that they satisfy one of three sets of constraints: (1) $V_{12} = V_{13}$, $V_{23} = 0$, $|\mathbf{a}| = |\mathbf{b}|$, and $\mathbf{a} \cdot \mathbf{b} = 0$, (2) $V_{13} = V_{23}$, $V_{12} = 0$, $|\mathbf{a}| = |\mathbf{a} + \mathbf{b}|$, and $\mathbf{a} \cdot (\mathbf{a} + \mathbf{b}) = 0$, or (3) $V_{12} = V_{23}$, $V_{13} = 0$, $|\mathbf{a} + \mathbf{b}| = |\mathbf{b}|$, and $(\mathbf{a} + \mathbf{b}) \cdot \mathbf{b} = 0$. When one of these sets of constraints is satisfied, only two of the three interference terms are present in Eq. (7), and the corresponding reciprocal wave vectors ($\mathbf{G}_{ij}$) are orthogonal and equal in magnitude. This plane group can emerge only if UCC-2 has been applied. Therefore, designs that satisfy the conditions above can always be optimized and exhibit unity absolute contrast ($V_{abs} = 1$). A typical interference pattern with *p4m* plane group symmetry is illustrated in Fig. 6 along with the corresponding design parameters. Figure 6 illustrates a design that results in unity absolute contrast ($V_{abs} = 1$) and an interference coefficient $V^{(2)} = 1/2$.

9. Plane Symmetry Group *p6m*

The *p6m* plane symmetry group is the highest symmetry group possible with three-beam-interference lithography. This plane group is characterized as having six unique reflection axes, three twofold symmetry points, three threefold symmetry points, and one sixfold symmetry point as shown in Fig. 1. This plane symmetry group can be realized only when plane wave parameters are chosen such that they satisfy the following set of constraints: $V_{12} = V_{13} = V_{23}$, $|\mathbf{a}| = |\mathbf{b}|$, and $\mathbf{a} \cdot \mathbf{b} = -0.5$. When this set of constraints is satisfied, all three interference terms are present in Eq. (7), and the corresponding reciprocal wave vectors ($\mathbf{G}_{ij}$) are equal in magnitude; one will bisect the other two, which lie at an angle of 120° with each other. This plane group can emerge only if UCC-1 has been applied. Therefore, designs that satisfy the conditions above can always be optimized and exhibit unity absolute contrast ($V_{abs} = 1$). A typical interference pattern with *p6m* plane group symmetry is illustrated in Fig. 7 along with the corresponding design parameters. Figure 7 illustrates a design that results in unity absolute contrast ($V_{abs} = 1$) and an interference coefficient $V^{(1)} = -1/3$.

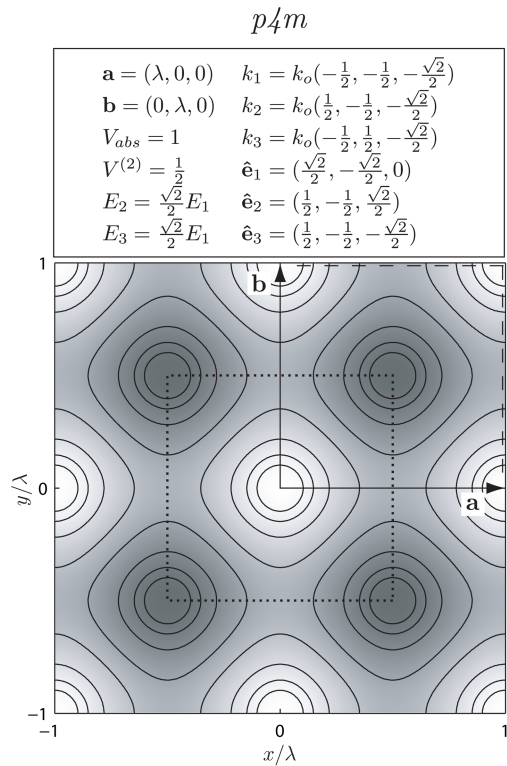The design in Fig. 7 illustrates one of the two fundamentally different interference patterns possible

p4m

$\mathbf{a} = (\lambda, 0, 0)$	$k_1 = k_o(-\frac{1}{2}, -\frac{1}{2}, -\frac{\sqrt{2}}{2})$
$\mathbf{b} = (0, \lambda, 0)$	$k_2 = k_o(\frac{1}{2}, -\frac{1}{2}, -\frac{\sqrt{2}}{2})$
$V_{abs} = 1$	$k_3 = k_o(-\frac{1}{2}, \frac{1}{2}, -\frac{\sqrt{2}}{2})$
$V^{(2)} = \frac{1}{2}$	$\hat{e}_1 = (\frac{\sqrt{2}}{2}, -\frac{\sqrt{2}}{2}, 0)$
$E_2 = \frac{\sqrt{2}}{2} E_1$	$\hat{e}_2 = (\frac{1}{2}, -\frac{1}{2}, \frac{\sqrt{2}}{2})$
$E_3 = \frac{\sqrt{2}}{2} E_1$	$\hat{e}_3 = (\frac{1}{2}, -\frac{1}{2}, -\frac{\sqrt{2}}{2})$

Fig. 6. Design parameters and associated interference pattern exhibiting *p4m* plane group symmetry. The UCC-2 has been applied and absolute contrast maximized, resulting in unity absolute contrast ($V_{abs} = 1$), with zero intensity at intensity nulls. The conventional primitive unit cell (dashed lines) and the Wigner–Seitz proximity unit cell (dotted lines) are shown.

when UCC-1 is satisfied. In this particular case, intensity minima are located at the lattice points. Again, there exists another design such that intensity maxima are located at the lattice points. Particularly for this hexagonal lattice design, it is important to have a full understanding of the range of contrast possible. As discussed above, if we allow $V^{(1)} < 0$, unity absolute contrast is possible ($V_{abs} = 1$, $V^{(1)} = -1/3$), resulting in intensity minima at lattice points. However, it may be desirable for intensity maxima to be located at these points. Figure 8 illustrates the maximum contrast for the *p6m* plane group, for $V^{(1)} > 0$, as a function of the zenith angle of the recording wave vectors ($\mathbf{k}_i$).

Figure 8 suggests that the lowest optimized absolute contrast available to designers is 0.6, for $V^{(1)} > 0$, when UCC-1 is applied. This occurs when all three recording wave vectors are orthogonal, possessing a zenith angle $\theta = \tan^{-1} \sqrt{2} \approx 54.7°$. In fact, this is the lowest optimized absolute contrast for all configurations of recording wave vectors when UCC-1 is satisfied and absolute contrast is maximized for $V^{(1)} > 0$. This can be demonstrated through a nonlinear minimization algorithm to search for the configuration of recording wave vectors resulting in the lowest maximum absolute contrast.
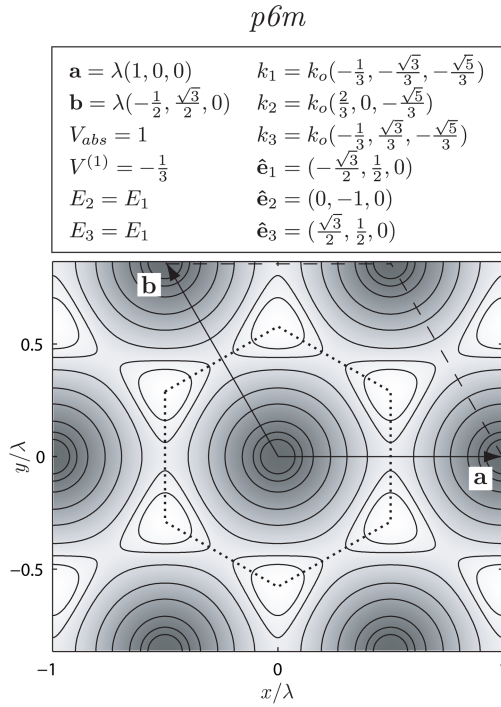
$p6m$

$$\mathbf{a} = \lambda(1, 0, 0) \qquad k_1 = k_o(-\tfrac{1}{3}, -\tfrac{\sqrt{3}}{3}, -\tfrac{\sqrt{5}}{3})$$
$$\mathbf{b} = \lambda(-\tfrac{1}{2}, \tfrac{\sqrt{3}}{2}, 0) \qquad k_2 = k_o(\tfrac{2}{3}, 0, -\tfrac{\sqrt{5}}{3})$$
$$V_{abs} = 1 \qquad k_3 = k_o(-\tfrac{1}{3}, \tfrac{\sqrt{3}}{3}, -\tfrac{\sqrt{5}}{3})$$
$$V^{(1)} = -\tfrac{1}{3} \qquad \hat{\mathbf{e}}_1 = (-\tfrac{\sqrt{3}}{2}, \tfrac{1}{2}, 0)$$
$$E_2 = E_1 \qquad \hat{\mathbf{e}}_2 = (0, -1, 0)$$
$$E_3 = E_1 \qquad \hat{\mathbf{e}}_3 = (\tfrac{\sqrt{3}}{2}, \tfrac{1}{2}, 0)$$

Fig. 7. Design parameters and associated interference pattern exhibiting $p6m$ plane group symmetry. This design results in one of two fundamentally different interference patterns when UCC-1 is applied, possessing intensity nulls at lattice points. Polarization unit vectors are coplanar (xy plane) and 120° apart from one another . The conventional primitive unit cell (dashed lines) and the Wigner–Seitz proximity unit cell (dotted lines) are shown.

10. Summary and Discussion

The relationships between the sets of constraints that result in the various plane groups discussed above can be determined when these constraints are viewed together. Figure 9 illustrates these rela-
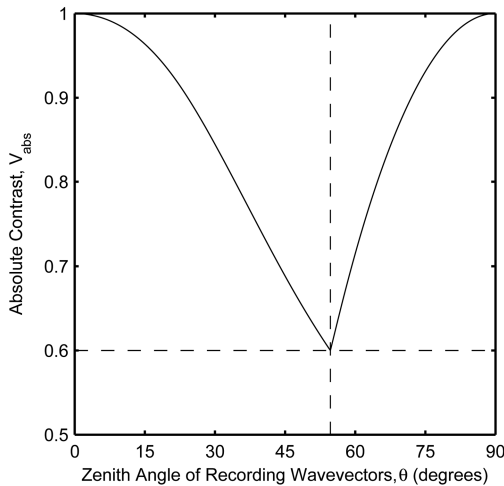

Fig. 8. Plot of maximum contrast obtainable for an interference pattern exhibiting $p6m$ plane group symmetry as a function of wave vector zenith angle when UCC-1 is applied and optimized for $V^{(1)} > 0$. The minimum occurs for $V_{abs} = 0.6$ at $\theta = \tan^{-1}\sqrt{2} \approx 54.7°$ or when all three recording wave vectors are orthogonal. The minimum shown, in actuality, is the global minimum for all configurations of three wave vectors.

tionships. As more restrictions are placed on the primitive basis vectors ($\mathbf{a}$ and $\mathbf{b}$) and interference coefficients (V_{ij}), other plane group symmetries emerge. In general, the interference of three arbitrary linear polarized plane waves will produce $p2$ symmetry. Figure 9 summarizes all the sets of constraints necessary to produce the other four plane symmetry groups and the relationships among them. This present methodology results in, at most, three sets of constraints (in terms of $\mathbf{a}$, $\mathbf{b}$, and V_{ij}) for each plane group. While single sets of constraints would result if the constraints were in terms of the reciprocal lattice vectors ($\mathbf{G}_{ij}$) and interference coefficients (V_{ij}), an intuitive understanding of the basis vectors ($\mathbf{a}$ and $\mathbf{b}$) and recording vectors ($\mathbf{k}_i$) would be more difficult to grasp. Moreover, the present methodology clearly demonstrates the opportunity for interference patterns with equivalent translational symmetries to exhibit different plane group symmetries.

Applying one of the two uniform contrast conditions and maximizing absolute contrast is a procedure to ensure that the designed interference pattern most accurately represents the translational symmetry of the desired lattice and results in a high-quality interference pattern. A second uniform contrast was introduced, and a complete description of uniform contrast was given. It is shown that unity absolute contrast ($V_{abs} = 1$) can always be achieved when either of the two uniform contrast conditions is applied and absolute contrast is maximized. This is
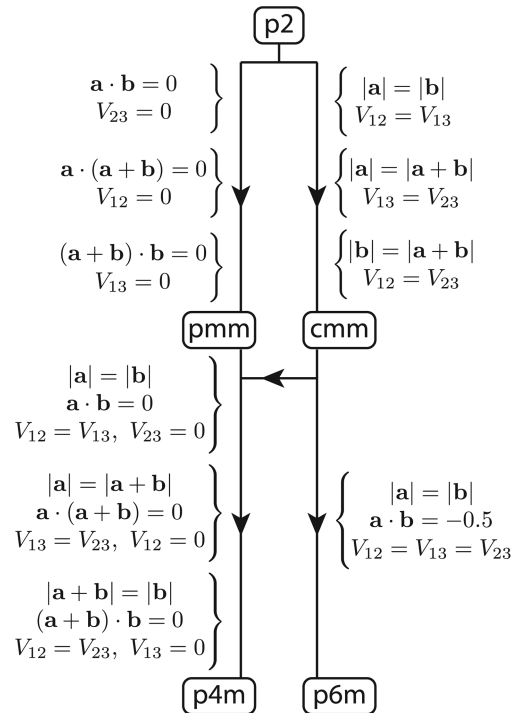

Fig. 9. Flow chart illustrating relationships between conditions required for each of the five plane symmetry groups to exist in three-beam interference. In general, $p2$ plane group symmetry occurs for general three-beam interference. As relationships between the basis vectors ($\mathbf{a}$ and $\mathbf{b}$) and interference coefficients (V_{ij}) emerge, the other four plane symmetry groups can exist.

very important to the success of holographic or lithographic processes. However, this can only be achieved for UCC-1 for $V^{(1)} < 0$, when intensity minima are located at lattice points. Finally, the lowest contrast available to designers when UCC-1 is applied and absolute contrast is maximized for $V^{(1)} > 0$ is $V_{abs} = 0.6$. This occurs when all three recording wave vectors are orthogonal to one another.

Adjustment of beam intensities and polarizations have a significant effect on the contrast and plane symmetry of three-beam-interference patterns. However, proper tuning of such can result in high-quality, symmetric motifs about lattice points for any configuration of three wave vectors.

References

1. T. K. Gaylord and M. G. Moharam, "Analysis and applications of optical diffraction by gratings," Proc. IEEE **75**, 894–937 (1985).
2. J. H. Moon, S. Yang, and S.-M. Yang, "Photonic band-gap structures of core-shell simple cubic crystals from holographic lithography," Appl. Phys. Lett. **88**, 121101 (2006).
3. G. Dolling, M. Wegener, C. M. Soukoulis, and S. Linden, "Negative-index metamaterial at 780 nm wavelength," Opt. Lett. **32**, pp. 53–55 (2007).
4. J. L. Stay and T. K. Gaylord, "Photo-mask for wafer-scale fabrication of two- and three-dimensional photonic crystal structures," in *Frontiers in Optics*, OSA Technical Digest (CD) (Optical Society of America, 2006), paper FThC5.
5. L. Z. Cai, X. L. Yang, and Y. R. Wang, "Formation of a microfiber bundle by interference of three noncoplanar beams," Opt. Lett. **26**, 1858–60 (2001).
6. M. Campbell, D. N. Sharp, M. T. Harrison, R. G. Denning, and A. J. Turberfield, "Fabrication of photonic crystals for the visible spectrum by holographic lithography," Nature **404**, 53–56 (2000).
7. M. Weidong, Z. Yongchun, D. Jianwen, and W. Hezhou, "Crystallography of two-dimensional photonic lattices formed by holography of three noncoplanar beams," J. Opt. Soc. Am. B **22**, 1085–1091 (2005).
8. L. Z. Cai, X. L. Yang, and Y. R. Wang, "Formation of three-dimensional periodic microstructures by interference of four noncoplanar beams," J. Opt. Soc. Am. **19**, 2238–2244 (2002).
9. T. Hahn, ed., *International Tables for Crystallography, Volume A: Space Group Symmetry* (Springer, 2002).